

# Coherent Diffraction of $\rho^0$ mesons off Au Nuclei at RHIC

STAR Collaboration  
(Dated: September 8, 2015)

The STAR Collaboration reports on the photoproduction of  $\pi^+\pi^-$  pairs in gold-gold collisions at a center of mass energy of 200 GeV/nucleon. These pairs are produced when a nearly-real photon emitted by one ion scatters from the other. The differential cross-section  $d\sigma/dt$  clearly exhibits a diffraction pattern, compatible with scattering from a gold nucleus, with 2 dips visible. We fit the  $\pi^+\pi^-$  mass spectrum to a combination of  $\rho^0$  and  $\omega$  resonances, plus a direct  $\pi^+\pi^-$  continuum; the ratio of  $\rho^0$  : direct  $\pi^+\pi^-$  is consistent with previous measurements in lighter systems. The  $\omega$  component is considerably larger than is expected from the measured  $\omega$  photoproduction cross-section and  $\omega \rightarrow \pi^+\pi^-$  branching ratio, in accord with previous studies. This may be due to  $\rho/\omega$  mixing, since  $\omega \rightarrow \pi^+\pi^-$  is disallowed by G-parity.”

PACS numbers: 25.75.Dw, 25.20.Lj, 13.60.-r

Heavy ions circulating in high energy colliders exchange intense and short-lived photon fluxes due to their high  $Z\alpha$  value and the strongly Lorentz contracted electric fields. Once they overlap, the strong interactions obscure these electromagnetic interaction both in intensity and complexity. The photon flux in these glancing events (referred to as Ultra-Peripheral Collisions (UPC)) is well described within the Weizaker-Williams formalism [1].

For Au ions at RHIC energies, these exchanged photons have small virtuality ( $\langle Q^2 \rangle \sim 2 \times 10^{-3} \text{GeV}^2$ ). The dipole model which has been successful at describing many of the Deep Inelastic Scattering (DIS) measurements performed at HERA [2] is also applicable in the UPC environment. The exchanged photons appears as a combination of its Fock states, the simplest of them being a quark, anti-quark pair which, once on-shell, becomes the set of vector mesons ranging from the lightest one, the  $\rho^0$  to ones not yet measured like the Upsilon. Whenever the photon fluctuates into a  $\rho$  meson, the energy of the photon-nucleon system at RHIC extends from 2 to 60 GeV well into region where the  $\rho^0$  photo-production cross section measured at HERA increases slowly with center of mass energy due to the exchange of a different object possessing vacuum quantum number; the so called Pomeron [3]. In the UPC environment, the coherent coupling to the wave function of the whole target samples values of the fraction of the nucleon momentum of the order  $x \sim 0.01$ .

Because of the high photon flux these UPC events have a high probability to be preceded or followed by photon exchanges that excite one or both ions into Giant Dipole Resonances (GDR) which then decays by “evaporation” of mostly a single nucleon at beam rapidity and small transverse momentum, most of the time, that nucleon is a neutron [4]. As the time scale of the decay of a GDR is much longer than the time scale of  $\rho$  meson photo-production off the target ion, the GDR excitations can be considered as factorizable; and do not appear to influence the coherent diffraction reported in this report.

This letter reports the measurement of exclusive  $\rho$  meson photo-production in Ultra Peripheral Collisions between Au ions at RHIC with an emphasis on the coherent diffraction pattern made visible in its squared transverse momentum distribution. This high statistics measurement together with a rather simple procedure to eliminate backgrounds and separate the incoherent component, has provided a diffraction pattern with up to three well defined maxima. The location of these peaks is consistent with the  $\rho$  mesons interacting coherently with the entire Au nuclei. This measurement with  $\rho$  is a proof of principle for future measurements at the EIC which will be conducted with higher precision and control over the kinematics of the events. These measurements will use fluxes of  $J/\Psi$  mesons which have a better localized wave function in contrast to the  $\rho$  meson [5]

The  $\rho$  mesons studied in this letter were detected through their decay into charged pion pairs measured in the STAR Time Projection Chamber (TPC) [6] which covers pseudo-rapidities  $\eta$  ranging from -1.5 to 1.5. These pions are identified by the amount of ionization energy they deposit in the TPC gas volume. This deposited energy is sampled along the particle tracks up to 45 times, translating into good separation between pions and kaons or protons up to their respective rest masses. The high number of measurements along the tracks permits, as well, a measurement of the momentum with a resolution of  $\Delta p/p = 0.005 + 0.004p$  with  $p$  in [GeV/c].

The STAR detector also includes a Time Of Flight (TOF) system that surrounds the TPC in azimuth, and a smaller coverage in pseudo-rapidity  $|\eta| < 1$ . This detector is also part of the trigger that selects the UPC events but its full timing capabilities are not used in the present analysis. At higher rapidities, charged particles are detected with the Beam Beam Counter (BBC) formed with 18 scintillator tiles arranged around the beam pipe on both sides of the nominal interaction point (IP), these detectors cover a pseudo-rapidity window of  $2 < |\eta| < 5$ . All RHIC experiments have installed compact calorimeters at beam rapidity. These detectors have good reso-

lution to detect beam momentum neutrons. The STAR UPC program makes use of the two triggers described in [7]. The work reported here is based on events recorded using the so called UPC\_Main trigger which requires low activity in the TOF detector (at least two and no more than six hits), no charged particles detected in the BBC detectors and finally, showers in both ZDC detectors corresponding to at least the equivalent of one neutron with beam momentum or up to five beam momentum neutrons.

The STAR TPC is active during a time window that lasts for 35  $\mu\text{sec}$ . With the RHIC clock frequency at 9.38 MHz a TPC event may contain tracks from a previous or a later bunch crossing and form several vertices. Matching between tracks emanating from those vertices and signal in the TOF detector related to the trigger is used to select the triggered vertex.

The data was collected during the RHIC run 10 which had Au beams circulating in the machine at 100 GeV/c. The total integrated luminosity for all runs included in this analysis reached  $1074.6 (\mu\text{b})^{-1}$  and yielded a sample of some 384K events with clean  $\rho^0$  meson candidates in events triggered with the UPC\_Main trigger. Events were selected to have signal in the ZDC calorimeters consistent with a shower produced by one and up to five beam neutrons. Pairs of tracks with opposite and equal charge originating from triggered vertices with only two tracks (exclusive events) were formed and stored in corresponding sets of histograms. The tracks in these pairs left ionization in the TPC volume consistent with them being pions (within three standard deviations of the expected value for all measured momenta). The number of samples recorded in those tracks should be greater than 14 and have a measured pseudo-rapidity in the interval  $|\eta| < 1.0$ . The z coordinate of the triggered vertex satisfies  $|v_z| < 50$  cm. Furthermore, both tracks on each pair are required to have a valid hit in the TOF detector. Finally, the invariant mass was calculated for the selected  $\rho^0$  meson candidates and a wide cut was applied such that  $0.25 < M_{\pi\pi} < 1.5$  GeV. Upper and lower limits of this mass cut are made more stringent in later stages of this analysis and are listed further ahead. This last condition, together with the BBC veto in the trigger produce the closest selection of exclusively photo-produced  $\rho$  mesons. The strongest background for this pion pair measurement is related to peripheral hadronic interactions where only a pair of the charged particles enters the TPC acceptance. Decays of the  $\omega$  meson into three pions, one of them neutral, is another source of background and  $K_s^0$  decays into opposite charge pions are also present in the data set, but are more abundant in incoherent events (higher pair transverse momentum). The best estimator for that background is usually constructed from equal charge pion pairs found in the same data set. The distribution of the transverse momentum of the  $\rho^0$  candidates is shown as a black histogram in Fig. 1 and the

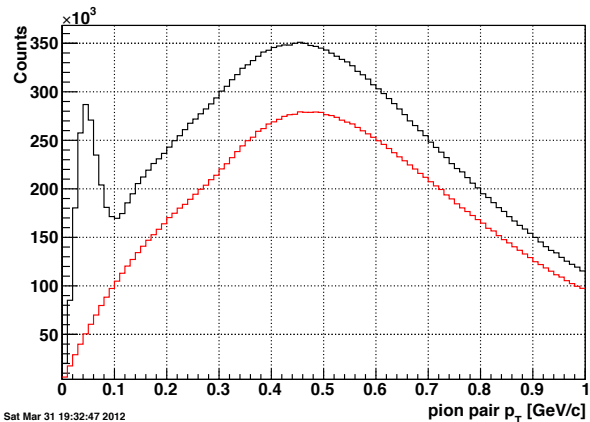


FIG. 1. The black histogram shows the distribution of the pion pair transverse momentum. The clear peak below 100 MeV/c is filled by the decay of coherently produced  $\rho$  mesons. The red histogram shows the distribution of the pair momentum for equal sign pion pairs. This distribution is considered the best approximation to the background in this measurement.

red histogram shows the corresponding distribution for pairs of equal charge. This second distribution is a good ansatz for the background present in events with such low multiplicity. The signal distribution has a prominent peak for pion pair transverse momentum smaller than 100 MeV/c. This peak is populated by events where the  $\rho^0$  meson scattered off the Au target as a whole i.e. coherently. The equal charge background shown in red in the figure, drops fast below the so called coherent peak and then grows with pair  $p_T$  to have a similar shape as the signal distribution which peaks broadly again around 400 MeV/c.

The overall  $\rho^0$  reconstruction efficiency used to correct for losses incurred along the full analysis chain has its biggest component in the geometrical acceptance defined by the coverage provided by the TOF detector and the lower momentum limits imposed by the solenoid magnetic field, as well as the track reconstruction efficiency, the vertex finding efficiency and the simulation of the trigger used to record the events used for this project. This correction has been estimated using pion pairs from simulated  $\rho$  mesons generated with the StarLight event generator [10]. In order to include the actual backgrounds present in the data, the pion pairs were transported through a full GEANT simulation of the STAR detector and later embedded in raw zero-bias events collected during data taking. Of particular interest for this report, the behavior of that correction as function of the transverse momentum squared  $-t$  of the  $\rho$  mesons has been found to be flat with a value of 6.4% (averaged over rapidity). In contrast, the same correction displayed as function of rapidity has a slightly asymmetric bell shape with a maximum at 13% at  $y$  0.15. The asymmetric shape

of this correction is well understood as being the result of an inefficient TPC sector on the East TPC side (negative rapidity). The same correction extracted as a function of the pion pair invariant mass has non-zero values starting at  $400 \text{ MeV}/c^2$  growing smoothly to saturate to a maximum value of 20% at mid-rapidity or  $\sim 9\%$  at higher rapidities.

Figure 2 shows the background subtracted invariant-mass of the selected pion pairs under the coherent peak

$$\frac{dN}{dM_{\pi^+\pi^-}} = \left| A_\rho \frac{\sqrt{M_{\pi\pi} M_\rho \Gamma_\rho}}{M_{\pi\pi}^2 - M_\rho^2 + i M_\rho \Gamma_\rho} + B_{\pi\pi} + C_\omega \frac{\sqrt{M_{\pi\pi} M_\omega \Gamma_\omega}}{M_{\pi\pi}^2 - M_\omega^2 + i M_\omega \Gamma_\omega} \right|^2 + f_p \quad (1)$$

where the momentum-dependent widths (expressed at  $q^2 = M_{\pi\pi}$ )  $\Gamma_\rho$  and  $\Gamma_\omega$  are written as:

$$\Gamma_\rho = \Gamma_0 \frac{M_\rho}{M_{\pi\pi}} \left( \frac{M_{\pi\pi}^2 - 4m_\pi^2}{M_\rho^2 - 4m_\pi^2} \right)^{3/2}$$

and  $\Gamma_\omega = \Gamma_0 \frac{M_\omega}{M_{\pi\pi}} \left( \frac{M_{\pi\pi}^2 - 9m_\pi^2}{M_\omega^2 - 9m_\pi^2} \right)^{3/2}$ . With  $\Gamma_0$  being the corresponding width for each meson. And  $f_p$  is a first order polynomial that could be needed to describe a remnant background.

The non-resonant component is shown with a dashed black line, the effect of the interference is shown with a blue dashed line, and finally the pure  $\rho^0$  yield extracted from the fit is shown with the red dotted line.

The lower limit in mass has been set at  $600 \text{ MeV}/c^2$  but it could be set at higher or lower values, the selection of this lower limit introduces a systematic error which is listed in Table I together with the best approximation to the shape of the correction function obtained with fits with polynomial of different order.

Figure 4 shows the fully corrected distribution of  $\rho^0$  mesons detected in events with only two tracks out of the triggered vertex and one to five neutrons in both ZDC calorimeters constructed with events selected by the UPC\_Main trigger. For each bin in rapidity, fits to the corresponding invariant mass distributions were performed to separate the resonant pion pairs from the flat non-resonant distribution. The integral of the pure Breit-Wigner function for masses ranging from 0.5 to 1.5 GeV is then used to extract a correction to the raw counts of  $\rho^0$  candidates. Finally, the resulting distribution has been scaled up by the full reconstruction efficiency as function of rapidity mentioned above. The systematic uncertainties identified for the measurement of this differential cross section are listed in Table II

Figure 5 shows the distribution of the Mandelstam variable  $t$  (with  $-t \sim p_T^{pair}$ ) for  $\rho^0$  candidates after background subtraction. The first peak of a coherent diffraction dominates the distribution at very small values of  $-t$ .

mentioned above. This distribution is fitted with a modified Söding parametrization [8], which includes the presence of a constant distribution in mass of non-resonant pion pairs as well as the presence of the  $\omega$  meson decaying into two charged pions as indicated in eqn. 1. The cross-section components corresponding to the  $\rho^0$  and  $\omega$  mesons are described with relativistic p-wave Breit-Wigner functions, both with real amplitudes  $A$  and  $C$ . The presence of non-resonant pions pairs is account with a real constant  $B$ :

The high  $-t$  side is filled by incoherent interaction with individual nucleons of the target ion. Such incoherent component is fit with a power law shape shown by the black curve in the figure. The parameter of the power law function are:  $A = 7.558 \pm 0.403$ ,  $p_0 = 0.485 \pm 0.057$ ,  $n = 3.35 \pm 0.20$   $\chi^2/NDF = 41/33$ . The incoherent cross-section is compared to a similar photo-production of  $\rho^0$  mesons at photon-proton center of mass energy of 78 GeV at HERA shown in Fig. 5 with black markers. Once that cross-section is scaled down by 60% to bring it to corresponding a RHIC  $\gamma$ -nucleon average energy, the two measurements overlap modulo a factor equal to 100, a value close to half of  $A$ . This comparison of nuclear and proton targets provides a tool to sample the nucleon distributions in Au as the ratio described above would range from a scaling by  $A$  for completely dilute systems to  $A^{1/3}$  in the so called ‘‘black disk’’ regime where incoherent interactions are strongly suppressed [13]. The integral of the fit to the incoherent component results in a value of cross section  $\sigma_{incoh} = 1.7 \text{ mb}$ .

The coherent component of the  $t$  distribution is then extracted by a simple subtraction of the power law fit.

Some discussion about the  $-t$  distribution and mention ALICE most recent publication at LHC [12].

Once the power law shape describing the incoherent component of the  $\rho$  meson scattering is subtracted from the  $-t$  distribution, the distribution is corrected for the compounded effects of tracking reconstruction and geometrical acceptance, vertex finding efficiency and a finite track and TOF detector matching necessary extracted from the embedding exercise described above. This correction is flat in  $t$  and has an average value of 7.3% over all rapidity values. Finally the distribution is normalized by the luminosity integrated over all data runs used in this analysis. The resulting differential cross is shown in Fig. 6 where up to two well defined peaks can be seen as well as a hint of a third one at high  $-t$  where the number of counts drops substantially. An

<i>rapidity</i>	B/A Lower limit of fit	C/A Lower limit of fit	B/A fullChain fit	C/A fullChain fit
-1., -0.35	3.2%	6.3%	1.9%	4.9%
-0.35 -0.15	2.%	2.5%	3.4%	21.8%
-0.15, 0.15	3.%	8.1%	1.7 %	6.5%
0.15, 0.35	3.8%	8. %	1.3%	0.6%
0.35, 1.	3.7%	6.3%	1.8%	0.4%

TABLE I. Systematic uncertainties allocated to the B/A and C/A ratios. The fits to the pion pairs invariant mass are normally done from 600 MeV up to 1.3 GeV. Changing the lower limit does produce different values of the B/A, such changes ranged from 500, 550, 600 and 650 MeV. The mass fullChain corrections are used as smooth functions obtained from fits to embedding data. The choice of functions sets another systematic uncertainty and polynomials of third, fourth and fifth order were used to extract a systematic error.

<i>rapidity</i>	PID cut	Fit to efficiency	number of track hits	<i>normalization</i>	RELDIS (XnXn only)
-1., -0.5	8.%	0.25%	0.2%	10%	5%
-0.5 0.	5.%	0.25%	0.05%	10%	5%
0., 0.5	5.%	0.25%	0.05%	10%	5%
0.5, 1.	8.%	0.25%	0.2%	10%	5%

TABLE II. Systematic uncertainties allocated to the pion particle identification with  $dE/dx$  in the TPC, the extraction of the fullChain efficiency in the embedding project, the selection of good quality tracks and the normalization of all extracted distributions. The last column list the systematic uncertainty allocated to the event generator RELDIS used to scale the UPC\_Main cross section to the XnXn value. The different values of the uncertainties are listed in four wide rapidity bins.

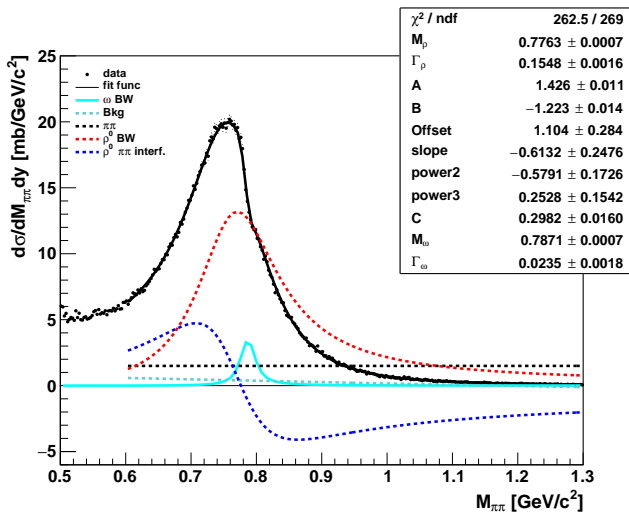


FIG. 2. The  $\pi^+\pi^-$  invariant-mass distribution for all selected  $\rho^0$  candidates at all values of rapidity within the STAR acceptance limited by the TOF detector ( $|y| < 1$ ). This high statistic sample of  $\rho^0$  mesons is displayed with small bin size (2.5 MeV) in order to highlight the presence of a substantial number of  $\omega$  mesons decaying into two charged pions and the resulting destructive interference. The black curve is the modified Söding function described in the text once fitted to the data in the range  $0.6 < M_{\pi\pi} < 1.3$  GeV. The  $\rho^0$  Breit-Wigner component of the fitted function is shown with a red-dashed curve and the constant non-resonant pion pair component is displayed with a black-dashed one. The interference between non-resonant pion pairs and the  $\rho^0$  meson is shown with a blue-dashed curve and a small third order polynomial shown with a cyan-dashed curve is used to account for a remnant background.

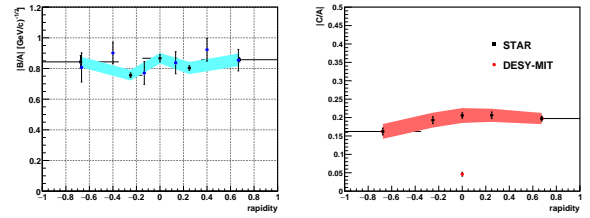


FIG. 3. The left panel shows the B/A ratio which compares the amplitudes of the non-resonant pion pairs (B) to that of the  $\rho^0$  meson. The right panel shows the C/A ratio which compares the amplitude of the  $\rho^0$  and the omega meson. The bands show the systematic uncertainties added in quadrature. The single red marker at rapidity 0 is the value measured at DESY [9] with photon bremsstrahlung on nuclear targets their best result  $\xi = 0.0106 \pm 0.0012$  is scaled by  $\sqrt{\Gamma_\rho/\Gamma_\omega}$ .

exponential function is used to extract the slope of the first diffraction peak the value of the slope is equal to  $386.6 \pm 59.8 (GeV/c)^{-2}$  and the location of the first dip is found to be at  $-t = 0.018 \pm 0.005 (GeV/c)^{-2}$  a second dip starts to form at  $0.043 \pm 0.01 (GeV/c)^{-2}$ . The separation between dipoles scales with  $1/(2R)^2$  with  $R = 6.4 \pm 1$  fm.

Around this section of the paper we will have a section to describe systematic uncertainties, we will list them as one coming from background subtraction, fit to power law with parameters fixed from other experiments. An overall systematic uncertainty is related to the luminosity and the inelastic cross section (10%) we may also quote some uncertainties on correction for efficiency and TOF match.

There will be discussion about calculations GDL [15]. In conclusion we will emphasize the ability of the

$-trange[(GeV/c)^2]$	track sel.	pion PID	Bkg sub.	Incoherent comp. sub.	Integrated luminosity	RELDIS
0 - 0.02	0.2%	8%	1.5	0.5%	10%	5%
0.02 - 0.04	0.2%	8%	1.5	1.0%	10%	5%
0.04 - 0.1	0.2%	8%	1.5	0.5%	10%	5%

TABLE III. An estimate for five systematic uncertainties identified in the generation of the  $-t$  distribution shown in Fig. 6 are shown as a per-cent of the measured cross-section in three ranges.

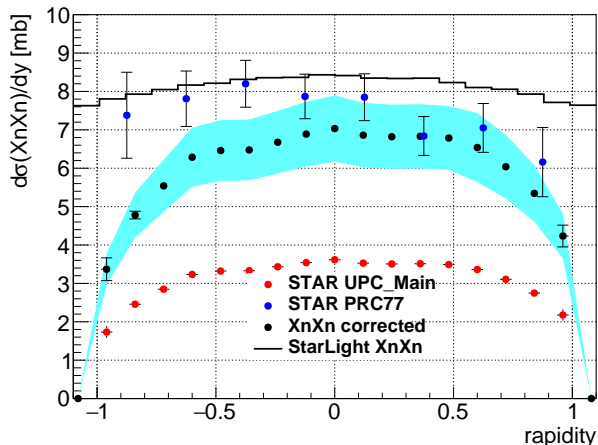


FIG. 4. Red markers show the cross-section as function of rapidity distribution for exclusively photo-produced  $\rho^0$  mesons reconstructed in events selected with the STAR UPC\_Main trigger. The black points show the same distribution scaled up to the full XnXn cross-section. The magnitude of the scaling was obtained using the RELDIS event generator (see text for details [11]). Statistical errors are shown with black vertical lines. The sum in quadrature of all systematic uncertainties identified for this measurement is shown with the cyan band. The blue markers show the same measurement performed by STAR in 2004 [7]. The rapidity distribution of XnXn StarLight events is shown with the black histogram.

STAR UPC program to study coherent diffraction with copiously photo-produced vector mesons. And add a summary.

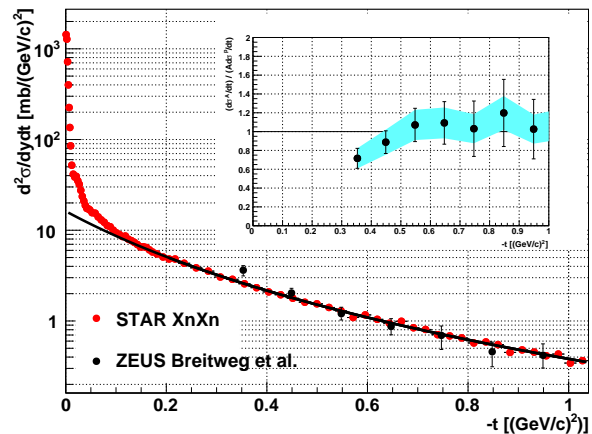


FIG. 5. The high  $t$  part of the distribution, which is dominated by the contribution from incoherent interactions is fit to a power law shape. The black points are proton-dissociation events measured by the ZEUS experiment at  $\gamma$ -proton center of mass energy of 78 GeV [14].

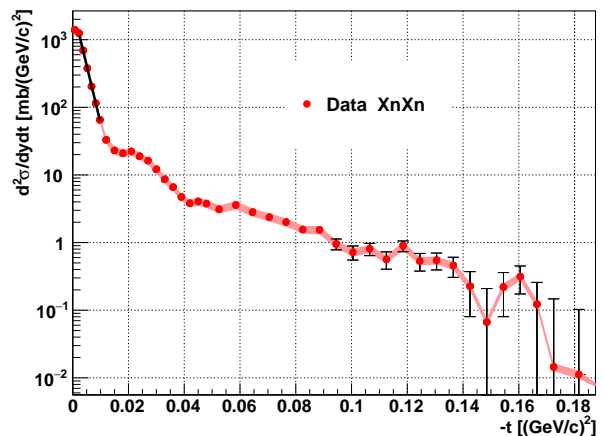


FIG. 6. Fully normalized coherent diffraction pattern for  $\rho^0$  mesons detected in exclusive XnXn events within a window in the vertex  $z$  coordinate of  $|V_z| < 50$  cm. The filled band shows the sum in quadrature of all systematic uncertainties listed in table III, the statistical errors are shown as vertical lines.

- [1] G. Baur, K. Hencken, D. Trautmann, S. Sadovsky, and Y. Kharlov, Phys.Rept. **364**, 359 (2002), arXiv:hep-ph/0112211 [hep-ph]
- [2] J. Bartels, K. J. Golec-Biernat, and H. Kowalski, Phys.Rev. **D66**, 014001 (2002), arXiv:hep-ph/0203258 [hep-ph]
- [3] J. Crittenden, (1997), arXiv:hep-ex/9704009 [hep-ex]
- [4] B. L. Berman and S. C. Fultz, Rev. Mod. Phys. **47**, 713 (1975)
- [5] T. Toll and T. Ullrich, Phys.Rev. **C87**, 024913 (2013), arXiv:1211.3048 [hep-ph]
- [6] M. Anderson, J. Berkovitz, W. Betts, R. Bossingham, F. Bieser, *et al.*, Nucl.Instrum.Meth. **A499**, 659 (2003),

- arXiv:nucl-ex/0301015 [nucl-ex]
- [7] B. I. Abelev *et al.* (STAR), Phys. Rev. **C77**, 034910 (2008), arXiv:0712.3320 [nucl-ex]
- [8] P. Soding, Physics Letters **19**, 702 (1966)
- [9] H. Alvensleben, U. Becker, W. Busza, M. Chen, K. J. Cohen, R. T. Edwards, P. M. Mantsch, R. Marshall, T. Nash, M. Rohde, H. F. W. Sadrozinski, G. H. Sanders, H. Schubel, S. C. C. Ting, and S. L. Wu, Phys. Rev. Lett. **27**, 888 (1971)
- [10] S. R. Klein and J. Nystrand, Phys. Rev. C **60**, 014903 (1999)
- [11] I. A. Pshenichnov, J. P. Bondorf, I. N. Mishustin, A. Ven-  
tura, and S. Masetti, Phys. Rev. **C64**, 024903 (2001),  
arXiv:nucl-th/0101035 [nucl-th]
- [12] J. Adam *et al.* (ALICE), (2015), arXiv:1503.09177 [nucl-  
ex]
- [13] T. Lappi and H. Mantysaari, Phys.Rev. **C83**, 065202  
(2011), arXiv:1011.1988 [hep-ph]
- [14] J. Breitweg *et al.* (ZEUS), Eur.Phys.J. **C14**, 213 (2000),  
arXiv:hep-ex/9910038 [hep-ex]
- [15] L. Frankfurt, M. Strikman, and M. Zhalov, Phys.Lett.  
**B537**, 51 (2002), arXiv:hep-ph/0204175 [hep-ph]
- [16] B. Abelev *et al.* (STAR), Phys.Rev.Lett. **102**, 112301  
(2009), arXiv:0812.1063 [nucl-ex]